# Generation of ultrafast terahertz radiation pulses on metallic nanostructured surfaces

**Gregor H. Welsh* and Klaas Wynne**

*Department of Physics, SUPA, University of Strathclyde, Glasgow G4 0NG, Scotland, UK*
**Corresponding Author:g.welsh@strath.ac.uk*
*http://bcp.phys.strath.ac.uk*

**Abstract:** A resonant "incoherent" rectification process is presented relying on the excitation of surface plasmons on a nanostructured metal surface. Excitation of gold and silver films with 800-nm femtosecond laser pulses results in the emission of terahertz radiation with an angle-dependent efficiency and an approximately third-order power dependence. It is shown that the source of this terahertz pulse generation is the surface-plasmon-assisted multiphoton ionization and ponderomotive acceleration in the evanescent field of the surface plasmon. Simple models are used to understand the forces and dynamics near the surface.



**OCIS codes:** (240.6680) Surface Plasmons; (320.7110) Ultrafast nonlinear optics

## References and links

1. C. A. Schmuttenmaer, "Exploring dynamics in the far-infrared with terahertz spectroscopy," Chem. Rev. **104**, 1759-1779 (2004).
2. A. Yariv, *Optical Electronics in Modern Communications* (Oxford University Press US, 1997), p. 768.
3. K. Wynne and J. J. Carey, "An integrated description of terahertz generation through optical rectification, charge transfer, and current surge," Opt. Commun **256**, 400-413 (2005).
4. A. Rice, Y. Jin, X. F. Ma, X. C. Zhang, D. Bliss, J. Larkin, and M. Alexander, "Terahertz Optical Rectification from (110) Zincblende Crystals," Appl. Phys. Lett. **64**, 1324-1326 (1994).
5. D. H. Auston, K. P. Cheung, and P. R. Smith, "Picosecond Photoconduction Hertzian Dipoles," Appl. Phys. Lett. **45**, 284-286 (1984).
6. D. Grischkowsky, S. Keiding, M. Vanexter, and C. Fattinger, "Far-Infrared Time-Domain Spectroscopy with Terahertz Beams of Dielectrics and Semiconductors," J. Opt. Soc. Am. B. Opt. Phys. **7**, 2006-2015 (1990).
7. J. J. Carey, R. T. Bailey, D. Pugh, J. N. Sherwood, F. R. Cruickshank, and K. Wynne, "Terahertz pulse generation in an organic crystal by optical rectification and resonant excitation of molecular charge transfer," Appl. Phys. Lett. **81**, 4335 (2002).
8. M. L. Groot, M. H. Vos, I. Schlichting, F. van Mourik, M. Joffre, J. C. Lambry, and J. L. Martin, "Coherent infrared emission from myoglobin crystals: An electric field measurement," P. Natl. Acad. Sci. USA **99**, 1323-1328 (2002).
9. X. M. Zheng, A. Sinyukov, and L. M. Hayden, "Broadband and gap-free response of a terahertz system based on a poled polymer emitter-sensor pair," Appl. Phys. Lett. **87**(2005).
10. X. C. Zhang, B. B. Hu, J. T. Darrow, and D. H. Auston, "Generation of Femtosecond Electromagnetic Pulses from Semiconductor Surfaces," Appl. Phys. Lett. **56**, 1011-1013 (1990).
11. E. Beaurepaire, G. M. Turner, S. M. Harrel, M. C. Beard, J. Y. Bigot, and C. A. Schmuttenmaer, "Coherent terahertz emission from ferromagnetic films excited by femtosecond laser pulses," Appl. Phys. Lett. **84**, 3465-3467 (2004).
12. D. J. Hilton, R. D. Averitt, C. A. Meserole, G. L. Fisher, D. J. Funk, J. D. Thompson, and A. J. Taylor, "Terahertz emission via ultrashort-pulse excitation of magnetic metal films," Opt. Lett. **29**, 1805-1807 (2004).
13. F. Kadlec, P. Kuzel, and J.-L. Coutaz, "Optical rectification at metal surfaces," Opt. Lett. **29**, 2674 (2004).
14. F. Kadlec, P. Kuzel, and J.-L. Coutaz, "Study of terahertz radiation generated by optical rectification on thin gold films," Opt. Lett. **30**, 1402 (2005).
15. M. Aeschlimann, C. A. Schmuttenmaer, H. E. Elsayedali, R. J. D. Miller, J. Cao, Y. Gao, and D. A. Mantell, "Observation of Surface-Enhanced Multiphoton Photoemission from Metal-Surfaces in the Short-Pulse Limit," J. Chem. Phys. **102**, 8606-8613 (1995).
16. H. L. Skriver and N. M. Rosengaard, "Surface energy and work function of elemental metals," Phys. Rev. B. **46**, 7157 (1992).
17. G. H. Welsh, N. T. Hunt, and K. Wynne, "Terahertz-pulse emission through laser excitation of surface plasmons in a metal grating," Phys. Rev. Lett. **98**, 026803 (2007).

#104605 - $15.00 USD Received 4 Dec 2008; revised 23 Jan 2009; accepted 30 Jan 2009; published 5 Feb 2009

18. S. E. Irvine and A. Y. Elezzabi, "Surface-plasmon-based electron acceleration," Phys. Rev. A. **73**, 013815 (2006).
19. J. Kupersztych and M. Raynaud, "Anomalous multiphoton photoelectric effect in ultrashort time scales," Phys. Rev. Lett. **95**, 147401 (2005).
20. J. Zawadzka, D. A. Jaroszynski, J. J. Carey, and K. Wynne, "Evanescent-wave acceleration of ultrashort electron pulses.," Appl. Phys. Lett. **79**, 2130 (2001).
21. H. Raether, *Surface Plasmons on Smooth and Rough Surfaces and on Gratings* (Springer-Verlag, 1988), Vol. 111, pp. 1-133.
22. E. D. Palik, *Handbook of Optical Constants of Solids* (Academic Press: San Diego, 1998).
23. R. A. Watts, T. W. Preist, and J. R. Sambles, "Sharp Surface-Plasmon Resonances on Deep Diffraction Gratings," Phys. Rev. Lett. **79**, 3978 (1997).
24. D. A. Jaroszynski, B. Ersfeld, G. Giraud, S. Jamison, D. R. Jones, R. C. Issac, B. M. W. McNeil, A. D. R. Phelps, G. R. M. Robb, H. Sandison, G. Vieux, S. M. Wiggins, and K. Wynne, "The Strathclyde terahertz to optical pulse source (TOPS)," Nucl. Instrum. Meth. A. **445**, 317 (2000).
25. M. C. Beard, G. M. Turner, and C. A. Schmuttenmaer, "Measuring Intramolecular Charge Transfer via Coherent Generation of THz Radiation," J. Phys. Chem. A., 878-883 (2002).
26. A. Gurtler, C. Winnewisser, H. Helm, and P. U. Jepsen, "Terahertz pulse propagation in the near field and far field," J. Opt. Soc. Am. A. **17**, 74-83 (2000).
27. A. E. Kaplan, "Diffraction-induced transformation of near-cycle and subcycle pulses," J. Opt. Soc. Am. B. Opt. Phys. **15**, 951-956 (1998).
28. J. L. Elechiguerra, L. Larios-Lopez, C. Liu, D. Garcia-Gutierrez, A. Camacho-Bragado, and M. J. Yacaman, "Corrosion at the nanoscale: The case of silver nanowires and nanoparticles," Chem. Mater. **17**, 6042-6052 (2005).
29. V. M. Shalaev, C. Douketis, J. T. Stuckless, and M. Moskovits, "Light-induced kinetic effects in solids," Phys. Rev. B. **53**, 11388-11402 (1996).
30. S. E. Irvine, A. Dechant, and A. Y. Elezzabi, "Generation of 0.4-keV femtosecond electron pulses using impulsively excited surface plasmons," Phys. Rev. Lett. **93**, 184801 (2004).
31. S. Bastiani-Ceccotti, P. Monchicourt, and T. Lehner, "Enhanced electronic emission by excitation of an interface resonance in metallic bilayer gratings irradiated by short laser pulses," Phys. Rev. B. **68**, 245411 (2003).
32. C. Toth, G. Farkas, and K. L. Vodopyanov, "Laser-Induced Electron-Emission from an Au Surface Irradiated by Single Picosecond Pulses at Lambda=2.94 Mu-M - the Intermediate Region between Multiphoton and Tunneling Effects," Applied Physics B-Photophysics and Laser Chemistry **53**, 221-225 (1991).
33. S. E. Irvine and A. Y. Elezzabi, "Ponderomotive electron acceleration using surface plasmon waves excited with femtosecond laser pulses," Appl. Phys. Lett. **86**(2005).
34. M. Kahl and E. Voges, "Analysis of plasmon resonance and surface-enhanced Raman scattering on periodic silver structures," Phys. Rev. B. **61**, 14078 (2000).
35. D. A. Turton, G. H. Welsh, J. J. Carey, G. D. Reid, G. S. Beddard, and K. Wynne, "Alternating high-voltage biasing for terahertz large-area photoconductive emitters," Rev. Sci. Instrum. **77**(2006).
36. G. H. Welsh, D. A. Turton, D. R. Jones, D. A. Jaroszynski, and K. Wynne, "200 ns pulse high-voltage supply for terahertz field emission," Rev. Sci. Instrum. **78**(2007).
37. R. Gomer, "Field-Emission, Field-Ionization, and Field Desorption," Surf. Sci. **300**, 129-152 (1994).
38. J. Zawadzka, D. A. Jaroszynski, J. J. Carey, and K. Wynne, "Evanescent-wave acceleration of femtosecond electron bunches," Nucl. Instrum. Meth. A. **445**, 324-328 (2000).
39. T. L. Gilton, J. P. Cowin, G. D. Kubiak, and A. V. Hamza, "Intense Surface Photoemission - Space-Charge Effects and Self-Acceleration," J. Appl. Phys. **68**, 4802-4810 (1990).

## 1. Introduction

Optical rectification is widely used to rectify ultrafast (picosecond or femtosecond) laser pulses from the visible (typically 800 nm) to the terahertz range. Such terahertz pulses find wide applications ranging from imaging to fundamental spectroscopy and the study of terahertz generation techniques.[1] The process of optical rectification has been known since the birth of lasers and nonlinear optics. One can usefully (although somewhat arbitrarily) make the distinction between incoherent and coherent optical rectification in which either a real or virtual intermediate state is involved.

*Coherent* optical rectification is a straightforward second-order nonlinear optical process in which the visible fields mix through the second-order susceptibility tensor to produce a terahertz (pseudo dc) field $E_{THz}(t) \propto \chi^{(2)} dI_{VIS}(t)/dt$,[2] which has a field shape approximately equal to the derivative of the envelope of the visible laser pulse.[3] Coherent optical rectification is typically performed in non-centrosymmetric crystals[4] such as ZnTe,

#104605 - $15.00 USD Received 4 Dec 2008; revised 23 Jan 2009; accepted 30 Jan 2009; published 5 Feb 2009

GaP, and $LiNbO_3$. In *incoherent* optical rectification, the visible laser pulses excite (real rather than virtual) charge carriers to a more mobile state in which charge acceleration leads to the emission of (coherent) radiation. The most well known example is the photoconductive Auston switch,[5] consisting of two dc-biased electrodes deposited on a semiconductor surface. Excitation of the semiconductor in the gap between the two electrodes by visible femtosecond laser pulses results in a current surge and the emission of a terahertz pulse.[6] It can be shown that the field of the emitted terahertz pulses in the far field is given by $E_{THz}(t) \propto d\vec{j}/dt$ where $\vec{j}$ is the (surface) current density.[3] However, there are other incoherent optical rectification processes. For example, it was shown that intra-molecular electron transfer can result in the emission of terahertz radiation.[1] Molecular electron transfer involves the movement of charge within a molecule, which constitutes a microscopic current. If the molecules are aligned in some way, the microscopic currents add up to a macroscopic current resulting in the emission of terahertz radiation. This was achieved in solution by applying a dc bias field aligning dipolar dye molecules,[1] in crystals by using chiral dye molecules[7] or proteins,[8] and in polymer films and protein films by poling.[9]

Numerous experiments have observed terahertz emission from surfaces. Early on, (unbiased) semiconductor surfaces were shown to be terahertz emitters as charge carriers may be excited in the surface depletion field of the semiconductor.[10] More recently, terahertz emission has been observed from ferromagnetic films[11, 12] and gold and silver surfaces.[13, 14] The latter was interpreted in terms of coherent rectification and is of particular interest here. However, the input power dependence of the terahertz fluence was shown to be fifth order.[13] In normal coherent optical rectification, the terahertz fluence should of course depend on the square of the input power. It is well known that gold and silver metal films irradiated with ultrashort visible laser pulses can exhibit the multiphoton photoelectric effect.[15] If terahertz emission in such metal films were related to the multiphoton photoelectric effect, one might expect an approximately eighth-order dependence of terahertz fluence on input power at 800 nm as the work function of gold and silver is 5.3 eV.[16] The metal surfaces used were not crystallographically flat and surface roughness can effectively lower the work function. It was also shown that there is a pronounced dependence of terahertz fluence $(\propto E_{THz}^2)$ on the thickness of the metal film used.[14] We recently showed that shallow gratings covered in gold films can be used to produce terahertz radiation.[17] These results suggest the involvement of surface plasmons (SPs) in the multiphoton photoelectric effect and subsequent terahertz radiation emission.

Here we will describe the generation from a metal coated shallow grating discussed previously,[17]. New data will be presented of terahertz pulse generation on this surface, the power dependence of terahertz-pulse generation, and its dependence on the metal used and other parameters. The results will be explained in terms of the excitation of SPs. The excitation of SPs results in the enhancement of the 800-nm excitation field and an evanescent field extending perpendicular to the metal surface. This results in ponderomotive acceleration of the photoelectrons[18-20] and consequently emission of terahertz radiation.

## 2. Sample preparation & experimental setup

Terahertz emission experiments have been performed on a number of nanostructured surfaces in order to characterize the role of SP excitation on the emission process. A shallow grating was obtained commercially. This will be described briefly below. The experimental setup used to generate and detect terahertz radiation pulses is also described.

#104605 - $15.00 USD Received 4 Dec 2008; revised 23 Jan 2009; accepted 30 Jan 2009; published 5 Feb 2009

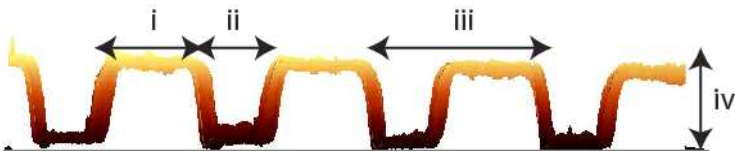


Fig. 1. (color online) Profile obtained by AFM of a shallow grating. i = 340 nm, ii = 160 nm, iii = 500 nm, and iv = 40 nm. The depth-to-pitch ratio is exaggerated, and the scan thickness is due to the image scans stacked across the surface.

*2.1 Metal over-layer coating*

An Edwards Coating System E306A was used for thermal vacuum evaporation of metals (using 1.0-mm diameter gold and 0.5-mm diameter silver wire, Goodfellow Cambridge) while the film thickness was measured with a Sycon Instruments STM-100/MF using a quartz crystal. The resultant surfaces were analyzed using a Witec Alpha atomic force microscope (AFM) operating in tapping mode.

*2.2 Surfaces used*

The shallow grating (made by Ibsen Photonics, Denmark) (Fig. 1)[17] consisted of a 10 × 10-mm$^2$ UV grade fused silica grating with a 500-nm period and a 40-nm etch depth as in Fig. 1. This relatively simple shallow grating was used in the hope that it would be straightforward to switch the effect of SP excitation on and off.

SPs are mixed electronic–electromagnetic excitations that are strongly localized on the interface of a metal and a dielectric.[21] The electromagnetic field of the SP falls off exponentially away from the interface. The effective refractive index of the SP (assuming the dielectric medium is air) is $n_{SP} = \sqrt{\varepsilon/\varepsilon+1}$, where $\varepsilon = n^2$ is the (frequency dependent) dielectric function of the metal. Using the known values of the refractive index of metals at 800 nm,[22] one finds for gold $n_{SP}$ = 1.018 + 0.0013 **i** and for silver $n_{SP}$ = 1.017 + 0.00092 **i**. Because the SP refractive index is larger than the index of air, SPs cannot be excited directly unless there is, for example, a surface corrugation. In the case of a grating, wavevector matching between bulk waves and SP waves can be achieved if the phasematching condition

$$\sin(\theta) + \frac{N\lambda}{\Lambda} = \mathrm{Re}(n_{SP}) \qquad (1)$$

is achieved.[21] Here $\theta$ is the angle of incidence of the laser beam onto the grating, $N$ is the diffraction order, $\lambda$ the (vacuum) laser wavelength, and $\Lambda$ the grating period. For the grating used in this work (500-nm pitch), one would then expect a resonance angle of 36° for both gold and silver. The 500-nm period means that for 800-nm excitation, only the zeroth diffracted order propagates while all other orders become evanescent. A 40-nm layer of gold or 45-nm layer silver is evaporated on the glass grating as this is where one would expect the sharpest and strongest SP resonance in the Kretschmann geometry.[21] More advanced electromagnetic calculations have shown that the angle and resonance width of the SP is influenced by the etch depth.[23]

An Ocean Optics USB2000 fiber coupled spectrometer was used for studying the angle dependent absorption of samples using an Ocean Optics LS1 white-light source. These were mounted in a custom-made setup to study both transmission through and reflection from a sample. This setup allowed the angle to be set at 2° increments and the propagation distance and sample position to remain constant. For reflection measurements, the sample was mounted in a central holder with the white light source and spectrometer mounted separately on the arms at either side of it. The position of each was then optimized over a small angle to give the maximum signal. A polarizer was also placed after the white light source for specific polarization measurements. The transmission regime involved the same apparatus set up linearly on an optical table.

#104605 - $15.00 USD Received 4 Dec 2008; revised 23 Jan 2009; accepted 30 Jan 2009; published 5 Feb 2009

*2.3 Experimental setup*

Terahertz-radiation emission experiments were carried out using a 1-kHz regenerative amplifier laser, capable of producing 1-mJ pulses centered at 800-nm with a pulse duration of 100-fs.[24] A schematic diagram of the experimental setup is shown in Fig. 2. The laser beam was split into two with about 98% used for pumping the samples and the remaining 2% for detection. The sample was excited with a 5-mm diameter collimated beam, which allowed for p-polarized or s-polarized excitation. The samples were mounted on a rotation stage and were be excited in transmission (with the metallic nanostructured surface facing away from the laser).

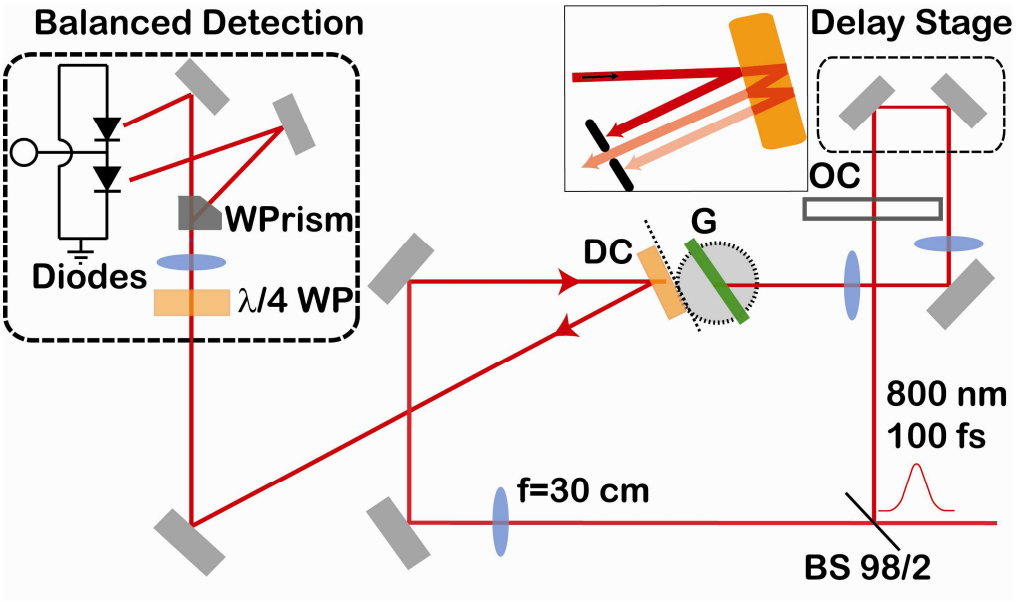


Fig. 2. (color online) Schematic diagram of experimental setup. BS, Beam Splitter; OC, Optical Chopper; G Grating on rotation mount; DC, 1-mm thick ZnTe Detection Crystal with black card to block pump light; WP Wave Plate; WPrism, Wollaston Prism. (Inset, center top) A schematic diagram of the correct reflection being selected by an aperture from the probe beam reflection.

The emitted terahertz radiation pulses were detected at a distance of 3 cm from the emitter by electro-optic sampling[3] using a 1-mm-thick <110>-cut ZnTe crystal in a reflection geometry as shown in Fig. 2. In this configuration, the 800-nm probe beam is focused by a 30-cm lens onto the detection crystal in a direction counter to that of the pump (and terahertz) beam. The detection crystal used has a wedged shape with the front and back surfaces at an angle of a few degrees. As a result, the reflected beam around 50 cm away consists of a number of spots of decreasing intensity corresponding to multiple reflections within the detection crystal (See Fig. 2 (inset)). The first and most intense spot is a reflection off the front surface of the crystal and contains no information. The second spot corresponds to a (single) reflection off the back surface. It contains two electro-optic sampling signals: one where the terahertz pulse is sampled while counter propagating and one where the terahertz and probe pulses co-propagate. As the phase delay experienced by a terahertz pulse in the 1-mm ZnTe crystal (~9.3 ps) is much larger than the terahertz pulse width (~1 ps), it can be shown that the counter-propagation signal is negligible compared to the co-propagation signal. Thus, only the second spot is re-collimated and passed through to a standard balanced detection setup allowing accurate measurement of the terahertz field shape. The advantage of this reflection setup[25] is greater accessibility to the sample.

#104605 - $15.00 USD Received 4 Dec 2008; revised 23 Jan 2009; accepted 30 Jan 2009; published 5 Feb 2009

It is well known that the terahertz field shape can alter dramatically on propagating from the near- to the far-field.[3, 26, 27] To achieve the best signal-to-noise ratio, it would be beneficial to measure in the near field, but since we want to rotate the sample, this is experimentally difficult. The relationship between the far-field and the separation $d$ between the generator and detector is given as $d >> r^2 / ct_0$ with $r$ the transverse radius of the pump beam and $t_0$ the full width half maximum of the terahertz transient.[2] In our experiment, $r^2 / ct_0 \approx 2cm$. It was confirmed in an independent experiment using this setup that the terahertz pulse shape changes with increasing distance and that a 3-cm distance between the generator and detector provides a far-field signal.

## 3. Experimental results

The work presented here has been inspired by reports of the generation of terahertz radiation by rectification on flat gold and silver surfaces.[13, 14] Unfortunately, we have not been able to reproduce these results within the signal-to-noise of our setup. In our experiments, 150-250 nm layers of gold were thermally evaporated under vacuum directly onto glass slides and used in the setup shown in Fig. 2 in reflection. Perhaps the signal is too weak to detect since the excitation of SPs would be very inefficient in such a nominally flat surface. These practical problems suggested the use of a transmission grating[17] as an efficient way of exciting SPs.[21]

### *3.1 Transmission grating*

Terahertz emission experiments were performed on the shallow grating described above (see Fig. 1). Fig. 3 shows the terahertz pulses produced when the grating is coated with 40 nm of gold or with 45 nm of silver. It can be seen that both pulses have similar characteristics to a pulse generated by optical rectification in a 0.5-mm thickness <110>-cut ZnTe crystal. The pulse duration is on the order of 1 ps in all three cases and the power spectrum extends to about 2.5 THz (limited by the 1-mm ZnTe detection crystal used[3]). The terahertz pulses shown in Fig. 3 were obtained at optimum conditions (angle of incidence 40° and 800-nm laser fluence 3.0 mJ/cm$^2$). The terahertz pulse produced in the gold-coated grating has a peak electric field which is about half of that of the pulse generated in ZnTe. The terahertz pulse produced in the silver-coated grating has a peak electric field 10× smaller still. The much smaller peak field obtained with the silver-coated grating is consistent with previous results[13] where the terahertz fluence from a silver surface was suppressed by two orders of magnitude. It is commonly assumed that this is caused by surface oxidation and the formation of sulfates.[28]

Experiments were performed to measure the terahertz fluence as a function of the 800-nm input power density. The terahertz fluence was calculated by fitting the data to an appropriate function[3] and squaring the amplitude obtained from the fit. Fig. 3 shows the power dependence obtained for terahertz pulses produced in a 0.5-mm ZnTe crystal and those produced on the gold- or silver-coated grating. The ZnTe data can be fit using a power law with a power of 1.8, which is consistent with the expected second-order optical rectification process. The data obtained using the gold-coated grating fits with a power of 3.2 although a better fit is obtained using two individual fits with powers of 3.5 at low incident fluence and 2.0 at higher fluence. The data obtained using the silver-coated grating fits with a power of 3.1. The incident laser power is limited to 3.6 mJ/cm$^2$ (on gold) and 3.0 mJ/cm$^2$ (on silver) by laser ablation of the metal from the grating. The incident power is limited to 3.0 mJ/cm$^2$ in the ZnTe crystal at which point multiphoton excitation and crystal damage occur. The inset of Fig. 3 shows the measured terahertz fluence for the grating structure coated with gold as a function of the coating thickness. Each measured point is for a 3.0-mJ/cm$^2$ excitation beam exciting the grating structure at an angle of incidence of 40°. This confirms that the maximum generation occurs when the structure is coated with 40 nm of gold.

#104605 - $15.00 USD Received 4 Dec 2008; revised 23 Jan 2009; accepted 30 Jan 2009; published 5 Feb 2009

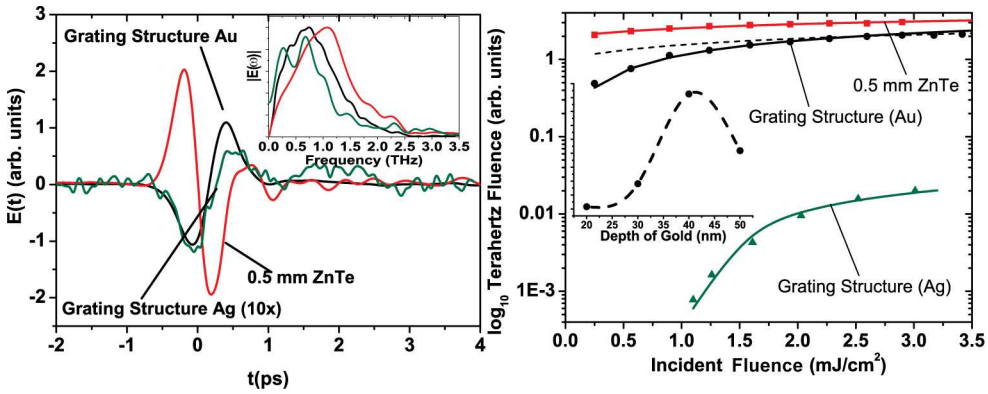


Fig. 3. (color online) (Left) Terahertz pulses emitted after excitation of the metal-coated grating shown Fig. 1 at an incident angle of 40° and an 800-nm laser fluence of 3.0 mJ/cm$^2$. Shown are measured terahertz pulses produced in the grating structure covered with 40-nm of gold and 45-nm of silver (multiplied by 10 times) and a comparison with a terahertz pulse produced in a 0.5-mm pathlength ZnTe crystal. The amplitudes of the three pulses are in arbitrary units but comparable. (inset) Normalized absolute value of the Fourier transform of the time domain traces. (Right) 800-nm pump laser-power dependence of the terahertz pulse fluence. At the top are the data obtained in a 0.5-mm length <110>-cut ZnTe crystal (squares) fit to a power law. Lower down are terahertz fluence data obtained using the shallow grating shown in Fig. 1 covered with 40-nm of gold (circles) or 45-nm of silver (triangles). The inset shows the measured terahertz fluence at an incidence angle of 40° for various depths of gold on the grating structure (the dashed line is a guide to the eye).

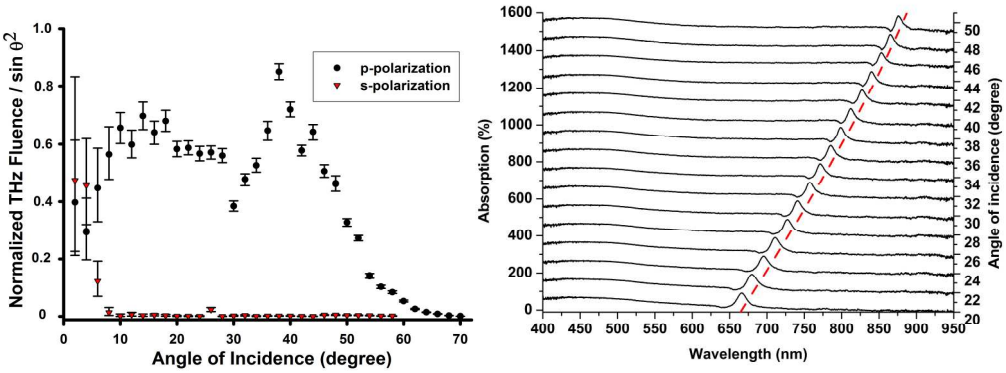


Fig. 4. (color online) (Left) The circles (triangles) show the normalized terahertz-pulse fluence *vs*. angle of incidence for the gold coated grating for p-polarized (s-polarized) excitation. (Right) Absorption spectrum obtained for a 50 nm gold coating on a 500 nm period grating substrate. Vertically offset by 100% for clarity. Also shown (dash) is the theoretical fit from (2) for a 500 nm period grating.

Shown in Fig. 4 is the angle dependence of the terahertz pulse fluence for *p* and *s*-polarizations on the external angle of incidence for the 800-nm 3.0-mJ/cm$^2$ laser radiation incident on the gold-coated grating. A similar result has been obtained with the silver-coated grating albeit at much reduced fluence. It is observed that the terahertz electric field changes sign on going from positive to negative angles. This shows that the electric field is polarized perpendicular to the surface. Therefore, in Fig. 4, the terahertz fluence has been divided by $\sin^2\theta$ to take account of the projection of the electric-field vector onto the propagation direction. The terahertz emission peaks at an angle of incidence of about 40° (in both gold and silver) for p-polarized excitation. When the excitation laser is s-polarized, terahertz emission is reduced by ~200×, the remaining signal likely caused by imperfect laser polarization. Terahertz emission can be seen at all angles of incidence.

#104605 - $15.00 USD Received 4 Dec 2008; revised 23 Jan 2009; accepted 30 Jan 2009; published 5 Feb 2009

In order to gauge the importance of SP excitation in the metal-coated grating, the angle-of-incidence dependent absorption in the visible and near infrared was measured using a p-polarized white light source (see Fig. 4). The grating was mounted and rotated as in the experiment and the transmitted and reflected intensity were used to obtain the absorption of the gold coating on the grating. The absorption is calculated by subtracting the transmitted and reflected intensities from the input intensity and expressing it as a percentage. As can be seen in Fig. 4 (the dashed line), the delocalized SP gives rise to an angle-dependent absorption (as described by Eq (1)) with a peak magnitude of about 80% at all angles.

The absorption is relatively constant as a function of angle only with the expected increase due to the excitation of surface plasmons. The absorption at shorter wavelengths is associated with absorption by the gold film itself. This is shown in Fig. 5, for the absorption of a 50 nm gold film on glass. Here the reflection spectrum is as expected for a gold coating with a high reflectivity (~90%) for part of the visible and near infrared regions. The transmission shows an increase at 500 nm tailing off to almost zero in the near infrared. The absorption shows ~55% absorption from 400-500 nm and this then reduces to around 10% at the laser wavelength of 800 nm.

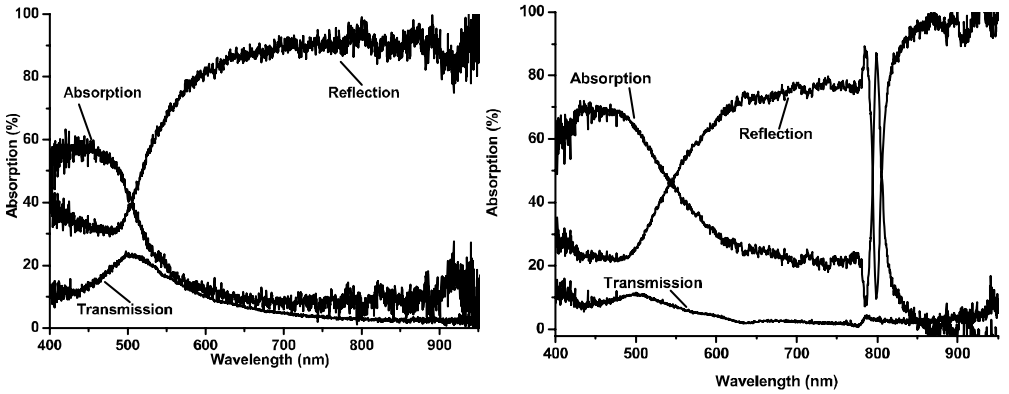


Fig. 5 (Left) Transmission, reflection, and absorption spectrum for a 50-nm gold coating on fused silica glass. (Right) Transmission, reflection, and absorption spectrum for a 50-nm gold coating on a 500-nm period grating substrate. Measured at an angle of incidence of 38°.

Figure 5 also shows the transmission, reflection, and absorption spectra this time for 50 nm of gold on the 500 nm grating. The absorption spectrum is the same as the vertically offset spectra in Fig. 4 for an incidence angle of 38°. By comparing both the absorption of a gold film and the absorption on the grating, the main differences are clearly seen. The 80% absorption due to the delocalized SP is evident at 800 nm. This component is also shown in transmission and more pronounced in the reflection spectra. The absorption is specific in that the FWHM is ~ 25 nm. For shorter wavelengths in the absorption spectrum, there is approximately a 10% increase in absorption and above 800 nm the absorption reduces to zero.

Fig. 6 shows the absorption of the grating at 800 nm as a function of the angle of incidence. When measured with a white-light source and a relatively high-resolution spectrometer, one can clearly observe a sharp peak at ~38° due the excitation of delocalized SPs. This would seem inconsistent with the broad peak observed in the angle dependence of terahertz generation shown in Fig. 4. The angle dependent absorption is also shown in Fig. 6 as measured with a low-power femtosecond laser (spectral width 25 nm FWHM). Because of the bandwidth of a femtosecond source, the angle dependent absorption is now convoluted with the laser spectrum much reducing the height of the SP resonance and increasing its width. The absorption at angles less than 38° may well be due to excitation of localized SPs through surface roughness in the gold film deposited on the grating. In comparing Fig. 6 with

#104605 - $15.00 USD Received 4 Dec 2008; revised 23 Jan 2009; accepted 30 Jan 2009; published 5 Feb 2009

Fig. 4, one should also take into account that at increasing angles of incidence, the power of the 800-nm excitation beam is spread out over a larger area and the incident intensity scales as $\cos(\theta)$. As optical rectification follows a power law with power 3.5, this would add an additional $\cos^{3.5}(\theta)$ dependence suppressing optical rectification at large angles.

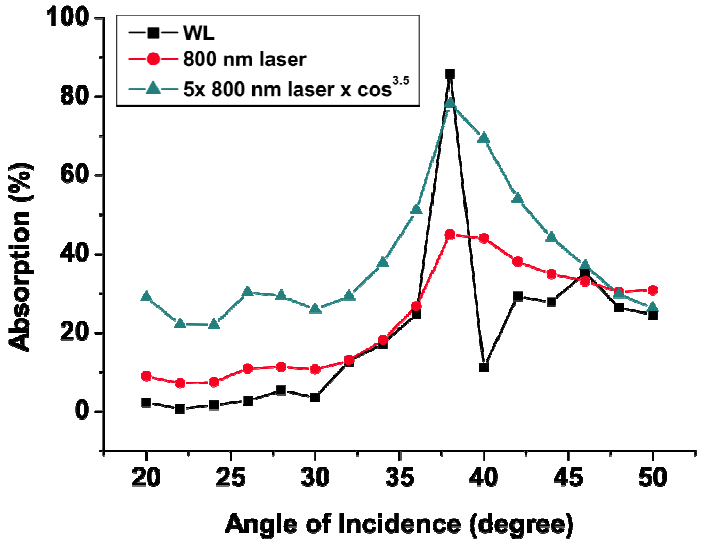


Fig. 6. (color online) Absorption at 800 nm as a function of angle of incidence for a 50-nm gold coating on a 500-nm period grating substrate. Shown are the absorption as measured with a white-light source and a spectrometer (squares) and that measured using an 800-nm femtosecond laser source (discs). Also shown (triangles) is the dependence when the incident intensity scaling of $\cos^{3.5}$ included.

## 4. Discussion and conclusion

It is clear that the optical-rectification process responsible for terahertz emission in the metallic nanostructured sample is not just a simple second-order process. The third- to fourth-order dependence of terahertz fluence on 800-nm incident fluence is inconsistent with that. Furthermore, the nonlinear optical process responsible is not a bulk but a surface process as the terahertz electric field is polarized perpendicular to the surface. The dependence of the emission on angle of incidence and on the input polarization imply the involvement of SPs either delocalized (through phasematched excitation according to Eq (1)) or localized (through surface roughness). This suggests that the optical rectification process is incoherent, involving the production of free electrons whose acceleration causes the emission of electromagnetic radiation.

It is well known that metallic films irradiated with high-power femtosecond laser pulses can emit photoelectrons in a process known as the nonlinear photoelectric effect.[15] The nonlinear photoelectric effect is enhanced by surface roughness[29] and by the excitation of surface plasmons, for example, in metal films on prisms[20, 30] or on gratings.[19, 31] The work function of gold and silver is 5.3 eV and 4.7 eV respectively.[16] Thus, in the perturbative regime and at 800 nm (1.5 eV), an electron would have to absorb four photons in order to overcome the work function. However, at high laser intensities, the laser field modifies the potential and the photoelectrons can tunnel out of the metal[32] reducing the effective order of the process. Thus, at intensities of about 0.1-1 GW/cm$^2$ a power of 3 to 4 has been observed,[15, 19, 31] while at higher intensities of about 1-100 GW/cm$^2$ the power-dependence has been seen to drop to 1.2–3. [33] The laser intensities used here are

#104605 - $15.00 USD Received 4 Dec 2008; revised 23 Jan 2009; accepted 30 Jan 2009; published 5 Feb 2009

comparable to the latter work. Moreover, the expected 800-nm field enhancement due to plasmon excitation is about the same in the Kretschmann prism geometry and the shallow grating used here.[34] Thus, based on this model one would expect that the high power 800-nm laser pulses produce a photocurrent $j \propto I_{800}^{n}$, where $n = 1.2–3$ resulting in a terahertz fluence $\left(E_{THz}\right)^2 \propto I_{800}^{2n}$ consistent with the observations.

Large area photoconductive terahertz antennas based on semiconductor switches,[5] accelerate conduction-band electrons with a dc bias field that is typically about 1 kV/cm. We have performed experiments applying a 10-kV dc bias field[35, 36] to the grating in vacuum and saw no difference in the strength or shape of the emitted terahertz pulse. Therefore, it is interesting to consider the forces and fields that cause (tunnel) emission of electrons. In the rectangular grating used here, SPs are localized on the corners of the grooves. However, from about a distance of 50 nm (approximately the groove depth) away from the grating top, the SP field becomes uniform and decays exponentially with a characteristic decay length $\lambda$ of about 500 nm.[34] It has been shown that the SP field (which oscillates at the laser frequency of 375 THz), gives rise to a ponderomotive force.[20, 31] The ponderomotive potential is $U_{pon}\left(z\right) = U_{final} \exp\left(-2z/\lambda\right)$, where $U_{final} = e^2 E_{SP}^2 / \left(4m\omega^2\right)$, $E_{SP}$ is the (time-dependent) amplitude of the 800-nm field on the surface, and $\omega$ is the laser angular frequency. From this expression, one can derive the ponderomotive force ( $F_{pon} = dU_{pon}/dz$ ) and an effective ponderomotive field ( $E_{pon} = F_{pon}/e$ ). The 800-nm laser field strength can be calculated using $E = \sqrt{2U/\left(\varepsilon_0 Ac\tau\right)}$, where $U$ is the pulse energy, $A$ is the beam area, and $\tau$ the pulse width. For a pulse energy of 1 mJ, a beam diameter of 5 mm and a pulse width of 100 fs, the laser electric field is about 1 GV/m. The field on the surface is enhanced by about a factor of 25, *i.e.*, $E_{SP} = 25$ GV/m when comparing the parameters of our grating with a previous study of enhancement values for surface-enhanced Raman scattering.[34] This results in $U_{final} = 5$ eV and $E_{pon} = 2 \times 10^7$ V/m. The calculated depth of the ponderomotive potential is too small, as experimentally measured maximum electron kinetic energies range as high as ~0.3 keV.[20, 30] This underestimation of the depth of the ponderomotive potential is probably caused by a combination of underestimating the SP-induced field enhancement and the neglect of space charge effects. The ponderomotive field is then estimated to be about 0.1 GV/m, which is close to the threshold for field emission.[37] Additionally, it is larger than a typical dc bias field as applied to a photoconductive antenna by two orders of magnitude.

The ponderomotive field is also larger than any conceivable coulombic field due to the attraction between the departing electron and the remaining hole. In the metal-coated grating, the charge of the hole will redistribute itself with the speed of light. As the photoelectrons only attain a maximum velocity of 0.2–3% of the speed of light (1–300 eV), Coulomb attraction will be irrelevant.

The terahertz pulses generated from both gold and silver layers on the grating (Fig. 3) show a FWHM of ~500 fs. The laser pulse used to excite the samples has a FWHM of 100 fs. One would expect the emitted terahertz pulse to be of approximately the same duration as the excitation pulse envelope since electrons should only be emitted from the structure and accelerated in the ponderomotive potential during this time. The much greater duration of the terahertz pulses suggests an additional acceleration mechanism. A possibility is that the current density is sufficiently high near the surface that self acceleration of the electrons may occur after the laser pulse excitation.

The current density can be estimated using previous measurements of photocurrents induced by the ultrafast nonlinear photoelectric effect[38] where currents of around 1 nA have been measured for both gold and silver films at comparable incident intensities. Based on this work, it can be estimated that $10^7$ electrons are liberated per second. Previous studies of the nonlinear photoelectric effect have shown that the photoelectrons are accelerated to energies of 0.5 eV [20] to 20 eV[19] when a long pulse was used. Here it will be assumed that the

#104605 - $15.00 USD Received 4 Dec 2008; revised 23 Jan 2009; accepted 30 Jan 2009; published 5 Feb 2009

average energy is 1 eV. The velocity is calculated by $v = \sqrt{2Ee/m}$, giving an electron drift velocity of $5.9 \times 10^7$ cm s$^{-1}$. The volume required to calculate the current density is taken as the laser cross section times the spatial extent of the laser pulse. This way a peak current density of 203.7 A/cm$^2$ is calculated. Previous electron dynamics simulations[39] have shown that at such current densities significant self acceleration can take place. That is, a cloud of electrons accumulates near the surface, which rapidly expands through coulomb repulsion giving rise to acceleration of electrons to several eV. This acceleration process can of course continue after the laser excitation pulse has died away, explaining the relatively long duration of the electromagnetic (terahertz) pulse produced.

In conclusion, it has been shown that incoherent optical rectification takes place in nanostructured metal surfaces through the excitation of SPs and evanescent-wave acceleration of photoelectrons resulting in an ultrafast photocurrent that radiates a terahertz pulse. The shallow grating used shows strong terahertz emission and is competitive with the inorganic crystal ZnTe. It may be possible to improve the efficiency of terahertz radiation production by optimizing the surface. For example, certain nanostructures enhance an externally applied dc field and may be used to boost the evanescent field associated with the SP.

**Acknowledgments**

We gratefully acknowledge funding for this project from the Engineering and Physical Sciences Research Council (EPSRC) and the Leverhulme Trust.

#104605 - $15.00 USD Received 4 Dec 2008; revised 23 Jan 2009; accepted 30 Jan 2009; published 5 Feb 2009